Kinetics of Amphiphile Association with Two-Phase Lipid Bilayer Vesicles

Antje Pokorny,* Paulo F. F. Almeida,* Eurico C. C. Melo,† and Winchil L. C. Vaz*
*Universidade de Coimbra, Departamento de Química, 3049 Coimbra Codex, and †Instituto de Tecnologia Química e Biológica, 2780 Oeiras, Portugal

ABSTRACT We examined the consequences of membrane heterogeneity for the association of a simple amphiphilic molecule with phospholipid vesicles with solid-liquid and liquid-liquid phase coexistence. To address this problem we studied the association of a single-chain, fluorescent amphiphile with dimyristoylphosphatidylcholine (DMPC) vesicles containing varying amounts of cholesterol. DMPC bilayers containing 15 mol% cholesterol show a region of solid–liquid-ordered (s-ℓ_o) coexistence below the T_m of pure DMPC (23.9°C) and a region of liquid-disordered–liquid-ordered coexistence (ℓ_d-ℓ_o) above the T_m. We first examined equilibrium binding and kinetics of amphiphile insertion into single-phase vesicles (s, ℓ_d, and ℓ_o phase). The data obtained were then used to predict the behavior of the equivalent process in a two-phase system, taking into account the fractions of phases present. Next, the predicted kinetics were compared to experimental kinetics obtained from a two-phase system. We found that association of the amphiphile with lipid vesicles is not influenced by the existence of ℓ_d-ℓ_o phase boundaries but occurs much more slowly in the s-ℓ_o phase coexistence region than expected on the basis of phase composition.

INTRODUCTION

Important membrane processes such as the insertion of proteins, transport of ions and proteins, and cell signaling require meticulous control at the membrane level to ensure normal cell function. In most cases, not only the final state but also the temporal scale on which these processes occur are important. Many of the peptides involved in signaling, for example, are amphipathic structures, and the entire class of lipid-linked proteins shares this feature. Thus the kinetics of insertion of amphiphiles into bilayers is probably an important aspect of the function of these cell components in a biological membrane. The possibility that lipid phase separations exist in biological membranes raises some interesting questions about their role in the control of such processes (Vaz and Almeida, 1993). Over the past decade, evidence has been accumulating in support of the view that a biological membrane is a chemically heterogeneous system and that heterogeneity may be an important requirement for normal cell function (Brown and Rose, 1992; Lisanti et al., 1994; Mayor and Maxfield, 1995; Simons and Ikonen, 1997; Edidin, 1997; Hwang et al., 1998), although this view has not remained uncontested (Kurzchalia et al., 1995; Kenworthy and Edidin, 1998). Our group has been contributing to the discussion about possible implications of membrane heterogeneity for membrane related processes, considering basic physical-chemical principles (Vaz, 1994, 1995, 1996; Melo et al., 1992; Vaz and Almeida, 1993; Thompson et al., 1995).

Membrane heterogeneity may be of various types. Over the years several lipid lamellar phases that may also exist in biological membranes have been clearly identified and characterized; lipid bilayers can exist as highly ordered solid (gel) phases (s phase), highly disordered fluid phases (ℓ_d phase), or relatively ordered fluid phases, which are often rich in cholesterol (ℓ_o phase). Under the appropriate conditions a lipid bilayer can exist as either one of these phases or as a mixture of coexisting phases.

Studies of systems showing solid-liquid phase separation have given rise to the idea that the interfaces present in such systems may also play a role in biological processes such as membrane protein insertion and in the regulation of membrane permeability. For example, the observation of an increased permeability to polar solutes in one-component lipid bilayers around the phase transition temperature, T_m, has been attributed to acyl-chain packing mismatch between s and ℓ_d phases that coexist at the T_m (Papahadjopoulos et al., 1973; Marsh et al., 1976; Cruzeiro-Hansson and Mouritson, 1988). Similarly, it has been shown that the permeability of lipid headgroup analogs in two-component, two-phase lipid bilayers is proportional to the amount of interface between the s and ℓ_d domains (Clerc and Thompson, 1995).

Fluid phase immiscibility, which is probably more relevant from a biological perspective, has clearly been shown to occur in some binary phospholipid mixtures (Wu and McConnell, 1975; Welti and Glaser, 1994) and has been particularly well studied in mixtures of phospholipids with cholesterol (Ipsen et al., 1987; Sankaram and Thompson, 1990, 1991; Vist and Davis, 1990). For example, the presence of more than ~5 mol% cholesterol in dimyristoylphosphatidylcholine (DMPC) bilayers leads to the formation of a cholesterol-rich ℓ_o phase, which can coexist with an ℓ_d phase above the T_m of pure DMPC (23.9°C) or with an s phase below the T_m (see Fig. 1). In the ℓ_d phase the cholesterol molecule is believed to be located in the membrane core region, spanning the acyl chain region in both monolayers, whereas in the ℓ_o phase the cholesterol mole-

Received for publication 9 June 1999 and in final form 15 September 1999.
Address reprint requests to Dr. Winchil L. C. Vaz, Universidade de Coimbra, Departamento de Química, P-3049 Coimbra Codex, Portugal. Tel.: 351-39-824-861; Fax: 351-39-827-703; E-mail: wvaz@ci.uc.pt.

0006-3495/00/01/267/14 $2.00

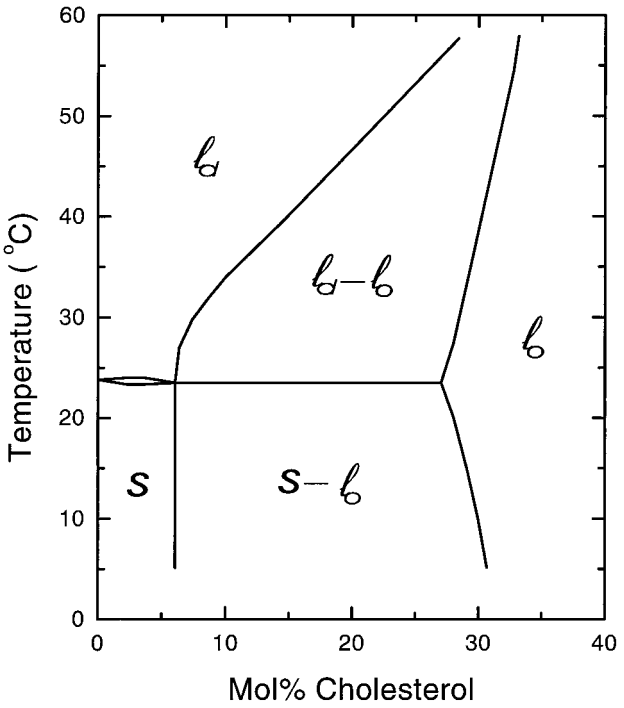

FIGURE 1 DMPC/cholesterol phase diagram. *s*, solid phase; ℓ_d, liquid-disordered phase; ℓ_o, liquid ordered phase. Data were taken from Almeida et al. (1992a) and Sankaram and Thompson (1991).

cule is arranged in a manner analogous to that of the phospholipid molecules, in both leaflets (Sankaram and Thompson, 1990, 1991). In this context it is interesting that eukaryotic membranes contain extremely well-controlled amounts of cholesterol varying from as little as 6 mol% in the endoplasmic reticulum to more than 30 mol% in the plasma membrane (Cullis and Hope, 1985). Because mixtures of phosphatidylcholines with cholesterol exhibit a phase separation over a very large temperature-composition interval, it is tempting to speculate that lipid phase separations of that type play a functional role in biological membranes.

In the present work we examine the consequences of membrane heterogeneity for the association of a simple amphiphilic molecule with phosphatidylcholine : cholesterol vesicles exhibiting solid-liquid phase coexistence and liquid-liquid phase coexistence (ℓ_o-ℓ_d). To address the problem, we first measured the kinetics of association of a fluorescent amphiphile with single-phase vesicles. To the best of our knowledge, the rates of insertion of small amphiphiles into vesicles have never been measured directly, but rather have been calculated from the partition coefficient and the rate of desorption from vesicles (Nichols, 1985; Jones and Thompson, 1990; Wimley and Thompson, 1990). However, we believe the rate of insertion to be a possibly crucial parameter in the insertion of small proteins into biological membranes, for example, thus making a direct measurement and understanding of lipid on-rates desirable. We report here a direct measurement of the rates of insertion and desorption of a fluorescent amphiphile as a function of lipid phase composition. The results are analyzed from a kinetic and thermodynamic point of view.

The rates determined for insertion into and desorption from single-phase vesicles are then used to predict the behavior of the equivalent process in a two-phase system, taking into account the fractions of phases present. The predicted kinetics are compared to experimental kinetics obtained from a two-phase system. We find that association of the amphiphile with lipid vesicles is not influenced by the existence of ℓ_d-ℓ_o phase boundaries but occurs much more slowly in the s-ℓ_o phase coexistence region than expected on the basis of phase composition.

MATERIALS AND METHODS

Chemicals

DMPC was purchased in powder form from Avanti Polar Lipids, and cholesterol was from Serva Fine Biochemicals. U-6 (4-(*N,N*-dimethyl-*N*-tetradecylammonium)methyl-(7-hydroxycoumarin)chloride) was obtained from Molecular Probes Europe, B.V. Chloroform p.A. was from Merck, and all other chemicals were from Sigma Chemical Co. Lipids and other chemicals were used without further purification.

Preparation of large unilamellar vesicles

Cholesterol and DMPC were separately dissolved in chloroform to give a final concentration of 10 mM each. Appropriate amounts of these chloroform solutions were mixed in a round-bottomed flask and rapidly dried using a rotary evaporator (Heidolph VV2000) at 60–70°C to prevent demixing of the components. After lyophilization the lipid film was hydrated by the addition of buffer preheated to at least 50°C to give a final lipid concentration of 10 mM. Swirling of the flask yielded a turbid suspension of multilamellar vesicles that was subsequently extruded ~10 times through two stacked Nuclepore polycarbonate filters of 0.1 μm pore size. Extrusion was performed at 50°C with a water-jacketed high-pressure extruder from Lipex Biomembranes. The LUV suspension obtained in this fashion was subjected to several cooling and heating cycles to ensure annealing of the lipid phases. The suspension was diluted in buffer to the desired concentration and used for fluorescence measurements. The buffer used in all experiments was 10 mM borate (pH 8.5), 10 mM KCl, 0.01 mM EDTA, and 0.02% NaN_3. Lipid concentrations were assayed through reversed-phase high-performance liquid chromatography.

Fluorescence experiments

Steady-state fluorescence measurements were performed in a thermostatted Jasco FP-777 spectrofluorimeter. U-6 was added to the buffer from a 0.50 mM stock solution in ethanol. Binding curves were obtained by the addition of lipid vesicles to a 1.0 μM solution of U-6 and monitoring the change in fluorescence intensity at 480 nm, using an excitation wavelength of 385 nm. At lipid concentrations greater than 0.1 mM the fluorescence emission was corrected for the contribution of scattered light. Kinetic experiments were performed using a self-built fluorimeter with a T-geometry equipped with a rapid-mixing device (Hi-Tech). Equal volumes of an U-6 solution (5.0 μM) and a lipid suspension (100 μM) were rapidly mixed, and the time course of fluorescence was monitored. The sample was excited through a monochromator at 385 nm and a Schott UG5 filter.

Fluorescence emission was monitored through two sandwiched long-pass filters, Schott KV408 and KV418. Data were acquired at a sampling frequency of 1 kHz, using commercially available software.

The fluorescent probe U-6 (Fig. 2; Kraayenhof et al., 1993) is a single-chain amphiphile with a critical micelle concentration of ~20 μM (data not shown). In the ground state the hydroxycoumarin undergoes an acid-base equilibrium with a pK of ~7.3 in aqueous solution at 25°C. The basic form absorbs at around 395 nm, and the protonated one at 340 nm. In phosphatidylcholine vesicles the pK of the ground state is shifted to ~8.3. The excited state has a pK well below pH 2, so that at a pH > 4 emission occurs exclusively from the deprotonated state with a maximum at 480 nm. We took advantage of the pK shift of the ground-state absorption upon insertion into vesicles to obtain a difference signal that was used to monitor incorporation.

THEORY

Single-phase vesicles

For the association of a fluorescent probe, P, with lipid vesicles, V, composed of a single phase we can write a simple reaction scheme with the rate constants k^*_{on} and k_{off} for the on- and off-rate, respectively:

$$P + V \underset{k_{off}}{\overset{k^*_{on}}{\rightleftharpoons}} PV. \tag{1}$$

Determination of molecular rate constants

In reaction scheme 1 the rate of change of the concentration of probe in solution, [P], is given by

$$\frac{d[P]}{dt} = -k^*_{on}[V][P] + k_{off}[PV], \tag{2}$$

where [V] and [PV] are the concentrations of vesicles and probe bound to vesicles, respectively. Expressing [V] in terms of lipid concentration, [L], assuming 10^5 lipid molecules per vesicle, [V] = [L] × 10^{-5}, we obtain

$$\frac{d[P]}{dt} = -k^*_{on}[L]10^{-5}[P] + k_{off}[PL] = k_{on}[L][P] + k_{off}[PL]. \tag{3}$$

where [PL] is now the concentration of probe bound to lipid and $k_{on} = k^*_{on} \times 10^{-5}$. The concentration of vesicles remains constant throughout the experiment, so that $k_{on}[L]$ becomes a pseudo-first-order rate constant and the above equation integrates to

$$[P](t) = \frac{P_o(k_{off} + k_{on}[L]e^{-(k_{on}[L]+k_{off})t})}{k_{on}[L] + k_{off}}, \tag{4}$$

where P_o is the initial probe concentration. For the time course of fluorescence we then obtain

$$F(t) = F_o(Ae^{-k_{obs}t} + B), \tag{5}$$

where

$$k_{obs} = k_{on}(K_a[L] + 1), \quad A = \frac{P_o K_a[L](1 - y)}{K_a[L] + 1},$$

$$B = \frac{P_o(1 + yK_a[L])}{K_a[L] + 1}.$$

K_a is the association constant of probe with lipid (in terms of lipid concentration) and y is the fluorescence intensity of the probe in vesicles relative to the one in buffer.

Determination of the association constant K_a and the partition coefficient K_p

For low concentrations of probe, the probe molecules bind independently of each other to the lipid vesicles, so that

$$K_a = \frac{[PL]_{eq}}{[P]_{eq}[L]_{eq}} = \frac{k_{on}}{k_{off}}, \tag{6}$$

where $[P]_{eq}$, $[L]_{eq}$, and $[PL]_{eq}$ are the equilibrium concentrations in water of probe, lipid, and probe bound to lipid, respectively. The volume partition coefficient K_p is related to K_a as follows:

$$K_p = \frac{[PL]^L_{eq}}{[P]} = \frac{[PL]_{eq}}{[L]_{eq}\bar{V}^L_o[P]_{eq}} = \frac{K_a}{\bar{V}^L_o} \tag{7}$$

where $[PL]^L_{eq}$ is the concentration of probe bound to lipid with respect to lipid and $\bar{V}^L_o$ is the lipid molar volume accessible to the probe. $\bar{V}^L_o$ for each lipid phase as a function of temperature was estimated from the molecular areas of a DMPC molecule in the different phases (taken from Almeida et al., 1992a), assuming a constant length of the hydrophobic "tail" of 18 Å. K_a is then determined through titration of a dilute solution of probe in buffer with a vesicle suspension. At a given temperature the observed decrease in fluorescence, F, as a function of lipid concentration, [L], is

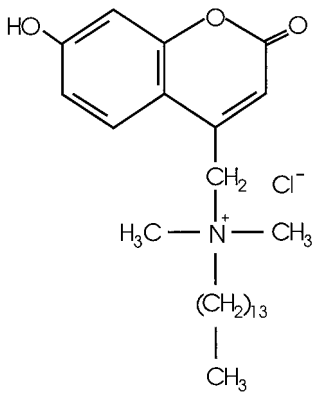

FIGURE 2 Chemical structure of U-6 (4-(*N,N*-dimethyl-*N*-tetradecylammonium)methyl-(7-hydroxycoumarin)chloride).

described by

$$F([\mathrm{L}]) = \frac{F_o(1 + yK_a[\mathrm{L}])}{1 + K_a[\mathrm{L}]}, \tag{8}$$

where F_o is the fluorescence of probe in buffer. A least-squares fit of the fluorescence kinetics to Eq. 5, therefore, directly yields k_{off} and, through the relation in Eq. 6, k_{on}.

Two-phase vesicles

For probe molecules, P, inserting into vesicles composed of two phases, a and b, with fractions f_a and f_b, we can construct the following reaction scheme:

$$\begin{array}{ccc} P + f_aV & \underset{k_{off}^{a}}{\overset{k_{on}^{a*}}{\rightleftharpoons}} & f_a\mathrm{PV_a}. \\ + & & \\ f_bV & & \\ k_{on}^{b*}\downarrow\uparrow k_{off}^{b} & & \\ f_b\mathrm{PV_b} & & \end{array} \tag{9}$$

In this case, the vesicle concentration is multiplied by the fractional amounts of each phase present, f_a or f_b, and the probe can interact with either phase a, forming the bound state PV_a, or with phase b, forming PV_b. Expressing the equations in terms of lipid concentration ($[V] = [L] \times 10^{-5} = k_{on}^{a*} \times 10^{-5} = k_{on}^{a}$, $k_{on}^{b*} \times 10^{-5} = k_{on}^{b}$ (compare Eq. 3), $f_b = 1 - f_a$, and [L] = constant), the coupled differential equations describing the system are

$$\begin{aligned} \frac{d[\mathrm{P}]}{dt} &= -(k_{on}^{a}[\mathrm{L}]f_a + k_{on}^{b}[\mathrm{L}](1 - f_a))[\mathrm{P}] + k_{off}^{a}f_a[\mathrm{PL_a}] \\ &\quad + k_{off}^{b}(1 - f_a)[\mathrm{PL_b}] \\ \frac{d[\mathrm{PL_a}]}{dt} &= k_{on}^{a}[\mathrm{L}]f_a[\mathrm{P}] - k_{off}^{a}f_a[\mathrm{PL_a}] \\ \frac{d[\mathrm{PL_b}]}{dt} &= k_{on}^{b}[\mathrm{L}](1 - f_a)[\mathrm{P}] - k_{off}^{b}(1 - f_a)[\mathrm{PL_b}]. \end{aligned} \tag{10}$$

This system of differential equations can be solved using matrix algebra (for a detailed explanation of the method, see Boas, 1983, and Gutfreund, 1995). From the solution of this system of rate equations we obtain the time courses of [P], $[PL_a]$, and $[PL_b]$:

$$\begin{aligned} [\mathrm{P}](t) &= -\frac{\alpha_1(\lambda_1 + k_{off}^{b} - k_{on}^{b}f_a)}{Lk_{on}^{b}(f_a - 1)}e^{\lambda_1 t} \\ &\quad - \frac{\alpha_2(\lambda_2 + k_{off}^{b} - k_{on}^{b}f_a)}{Lk_{on}^{b}(f_a - 1)}e^{\lambda_2 t} + \alpha_3 \\ [\mathrm{PL_a}](t) &= \frac{\alpha_1(\lambda_1 + k_{off}^{b} - k_{on}^{b}f_aL - k_{off}^{b}f)}{Lk_{on}^{b}(f_a - 1)}e^{\lambda_1 t} \\ &\quad + \frac{\alpha_2(\lambda_2 + k_{off}^{b} - k_{on}^{b}f_aL - k_{off}^{b}f)}{Lk_{on}^{b}(f_a - 1)}e^{\lambda_2 t} + \frac{\alpha_3 k_{on}^{a}L}{k_{off}^{a}} \\ [\mathrm{PL_b}](t) &= \alpha_1 e^{\lambda_1 t} + \alpha_2 e^{\lambda_2 t} + \frac{\alpha_3 k_{on}^{b}L}{k_{off}^{b}}. \end{aligned} \tag{11}$$

The time course of fluorescence expected for the system in Scheme 9 will thus be characterized by two apparent rate constants, $-\lambda_1$ and $-\lambda_2$. Both are a complex combination of all four molecular rate constants, the fractions of phases present, and the lipid concentration, but the faster apparent rate is dominated by the faster molecular rate (the on-rates) and the slower apparent rate by the off-rates:

$$\begin{aligned} \lambda_1 &= -1/2(k_{off}^{b} + k_{off}^{a}f_a - k_{on}^{b}Lf_a + k_{on}^{a}Lf_a \\ &\quad + k_{on}^{b}L - k_{off}^{b}f_a - \omega) \\ \lambda_2 &= -1/2(k_{off}^{b} + k_{off}^{a}f_a - k_{on}^{b}Lf_a + k_{on}^{a}Lf_a \\ &\quad + k_{on}^{b}L - k_{off}^{b}f_a + \omega), \end{aligned} \tag{12}$$

where

$$\begin{aligned} \omega = [&(1 - f_a)^2(k_{on}^{b}L + k_{off}^{b})^2 + f_a^2(k_{on}^{a}L + k_{off}^{a})^2 + k_{on}^{b\ 2}L^2 \\ &+ 2f_a(1 - f_a)(k_{on}^{a}k_{on}^{b}L^2 - k_{on}^{a}k_{off}^{b}L - k_{on}^{b}k_{off}^{a}L \\ &- k_{off}^{a}k_{off}^{b})]^{(1/2)}. \end{aligned}$$

The amplitude factors α_1, α_2, and α_3 are determined using the initial concentrations of P, PL_a, and PL_b. The time course of fluorescence for the incorporation of U-6 into two-phase vesicles will thus be given by

$$F(t) = F_o([\mathrm{P}] + y_a[\mathrm{PL_a}] + y_b[\mathrm{PL_b}]), \tag{13}$$

where y_a and y_b are the relative fluorescence intensities of probe in phase a and phase b, respectively.

RESULTS

Association of U-6 with single-phase vesicles: ℓ_d, ℓ_o, and s phases

We studied the insertion of U-6 into pure DMPC vesicles below and above the T_m and into DMPC vesicles containing 35 mol% cholesterol to obtain the kinetics of insertion into the *s*, ℓ_d, and ℓ_o phases, respectively. Fig. 3 *A* shows a typical binding curve obtained by titrating a 1 μM solution of U-6 at pH 8.5 with a suspension of lipid vesicles in the ℓ_d phase. K_a as a function of temperature from 12 to 42°C was determined by a nonlinear least-squares fit of the experimental binding curves to Eq. 8, using vesicles in the *s*, ℓ_d, and ℓ_o phases. These values of K_a were then used in the determination of the molecular rate constants k_{on} and k_{off} in

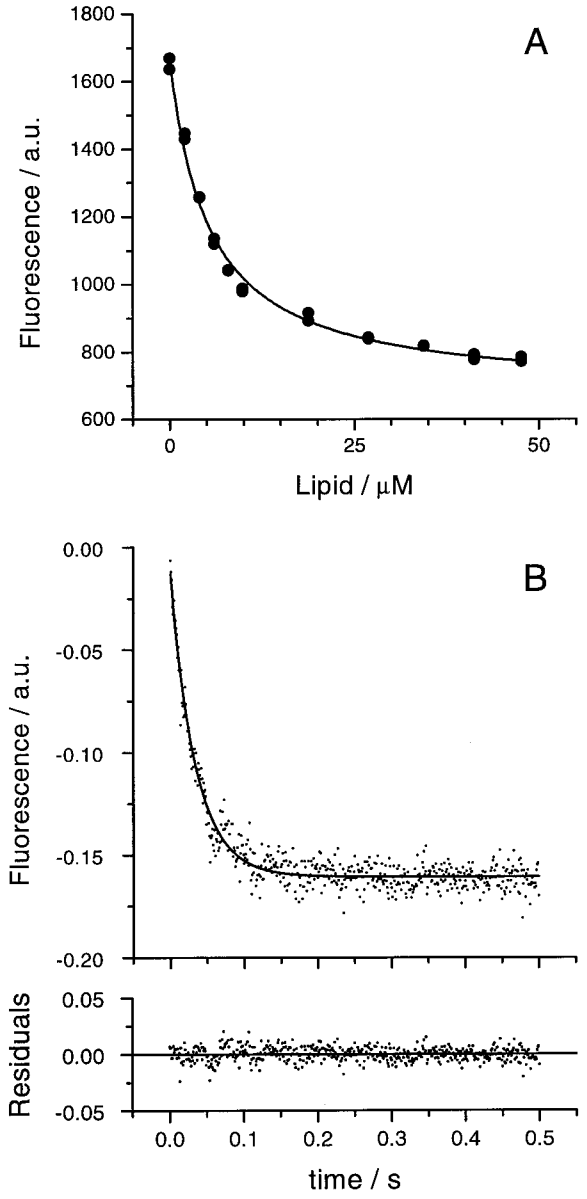

FIGURE 3 Single-phase vesicles. (*A*) Titration of a 1 μM solution of U-6 with a suspension of large unilamellar vesicles (LUVs) of pure DMPC at 30°C. The solid line represents a fit to the data according to Eq. 8. $K_a = 1.9 \times 10^5$ (with respect to lipid concentration). (*B*) Kinetics of insertion into pure DMPC LUVs at 30°C (ℓ_d phase). The solid line is a single exponential function with $\tau_{obs} = 34.06$ ms.

the kinetic experiments as described in Materials and Methods, Theory. Fig. 3 *B* shows typical fluorescence kinetics of U-6 insertion into ℓ_d-phase vesicles. The molecular rate constants obtained in this fashion are plotted in Fig. 4. It is of interest to point out that the traces obtained at temperatures close to the T_m (23–25°C) could not be described by a monoexponential fit (Fig. 4 *A*). The fits were clearly biexponential, indicating the presence of more than one phase on the time scale of the experiment and a considerable acceleration of the off-rate.

The standard Gibbs energy of transfer from water to membrane is given by $\Delta G^o = -RT \ln K_p$. The standard reaction enthalpies, ΔH^o, for the association of U-6 with vesicles in the *s*, ℓ_d, and ℓ_o phases were determined from the slope of a van't Hoff plot (Fig. 5, *A* and *D*) and the entropy term via $\Delta G^o = \Delta H^o - T\Delta S^o$.

The Gibbs energies of activation for the processes of insertion and desorption in the different phases can, in principle, be determined using the Eyring activated state theory, according to which

$$k = Ae^{-\Delta G^{\ddagger o}/RT}, \tag{14}$$

where R is the gas constant and T is the absolute temperature in Kelvins. To calculate the value of $\Delta G^{\ddagger o}$, however, we still need to know the preexponential factor A in Eq. 14, which has been estimated using a variety of models (Aniansson et al., 1976; Almeida, 1999). The drawback of that approach is that the magnitude of A and, consequently, $\Delta G^{\ddagger o}$ becomes highly model-dependent. However, if we consider the process of insertion, it turns out that A is given by k_{on} in the limit of $\Delta G^{\ddagger o} = 0$, which is, in fact, also the definition of a diffusion-limited on-rate. This quantity can be readily estimated according to Smoluchowski (1917):

$$k_o = 4\pi r_o D = A, \tag{15}$$

where r_o is the vesicle radius and D is the diffusion coefficient of a lipid molecule in water. We took D to be 5×10^{-6} cm^2/s at 20°C with an activation enthalpy of 5 kcal/mol (Jones and Thompson, 1990). It therefore becomes possible to estimate the magnitude of the preexponential factor for the on-rate, which must be the same for the off-rate, as dictated by the principle of microscopic reversibility.

Because the Gibbs energy of transfer of the amphiphile from water to the bilayer is proportional to ln K_p (not to ln K_a), we must also include the lipid molar volume in the determination of the Gibbs energies of activation. More precisely, we are interested in the on-rate per unit volume, which takes into account the variation of molecular lipid volume with lipid phase and temperature. Thus we write

$$\begin{aligned}\Delta G^o &= -RT \ln K_p = -RT \ln\left(\frac{k_{on}}{k_{off}\bar{V}_o^L}\right)\\ &= -RT[\ln(k_{on}/\bar{V}_o^L) - \ln k_{off}]\\ &= \Delta G_{on}^{\ddagger o} - \Delta G_{off}^{\ddagger o}\end{aligned}$$

$$\frac{k_{on}}{\bar{V}_o^L} = \frac{k_o}{\bar{V}_o^L}e^{-\Delta G_{on}^{\ddagger o}/RT}$$

$$k_{off} = \frac{k_o}{\bar{V}_o^L}e^{-\Delta G_{off}^{\ddagger o}/RT}. \tag{16}$$

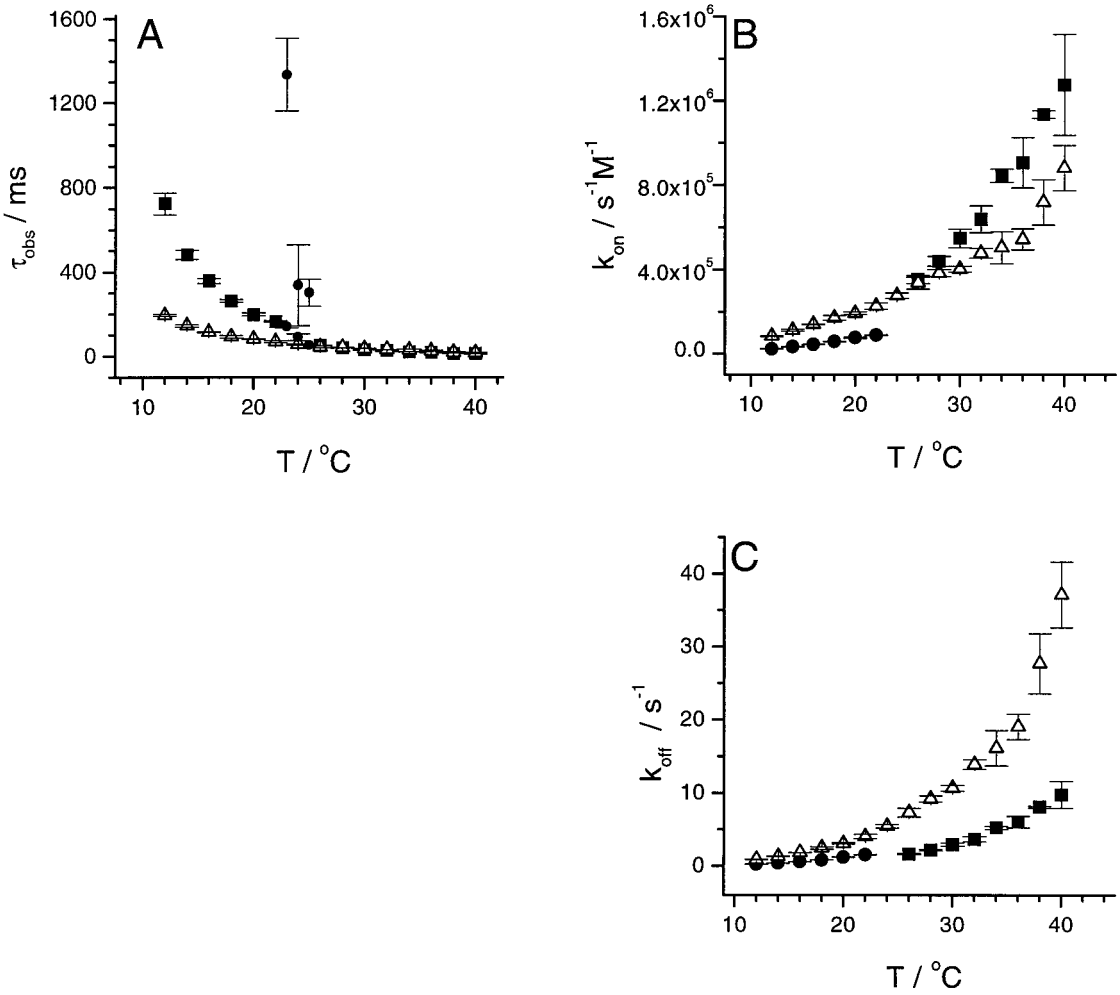

FIGURE 4 Single-phase vesicles. (*A*) Observed time constants (τ_{obs}) for the insertion of U-6 into *s*-, ℓ_d-, and ℓ_o-phase vesicles. ■, Monoexponential fit, pure DMPC. ●, Biexponential fit, pure DMPC (23, 24, 25°C). △, Monoexponential fit, DMPC : cholesterol 65 : 35. (*B*) The on-rates, k_{on}, into the *s*, ℓ_d, and ℓ_o phases as a function of temperature. (*C*) The corresponding off-rates, k_{off}. ●, *s* phase. ■, ℓ_d phase. △, ℓ_o phase. The error bars represent the standard deviation of six experiments.

The corresponding enthalpies of activation, $\Delta H^{\ddagger o}$, were then determined from the Arrhenius plots in Fig. 5, *B*, *C*, *E*, and *F*. The result of this analysis is summarized graphically in Fig. 6. Because the treatment is independent of a particular activated-state model, the absolute magnitudes of the thermodynamic quantities associated with the activated state are meaningful.

Association of U-6 with two-phase vesicles: regions of ℓ_d-ℓ_o and s-ℓ_o coexistence

In the analysis of the kinetics of association observed in the two-phase regions we used the data obtained from single-phase vesicles at each temperature without further adjustments and the fractions of phases as determined from the phase diagram to try to describe the experimental kinetics. The solid line in Fig. 7 *A* is a purely theoretical prediction for the kinetics of insertion into a region of ℓ_d-ℓ_o phase coexistence based on Eqs. 11–13. The kinetics are a function of 1) the fractions of the two phases present, 2) the total lipid concentration, 3) the relative fluorescence intensities of the probe in the two phases, and 4) the rates of insertion and desorption into the individual phases as determined from single-phase vesicles. The model predicts two apparent rate constants, $-\lambda_1$ and $-\lambda_2$, one of which is on the order of seconds and, therefore, does not contribute significantly to the observed kinetics on the millisecond time scale. On a fast time scale the kinetics are then determined by a single apparent rate constant, $-\lambda_2$, and we find that in the region of ℓ_d-ℓ_o phase coexistence, the value of $-\lambda_2$ coincides very well with the rate obtained from a monoexponential fit to the experimental data (Fig. 7 *A* and *high temperature points* in Fig. 7 *C*). Interestingly, we find that the traces obtained at temperatures close to the solidus line

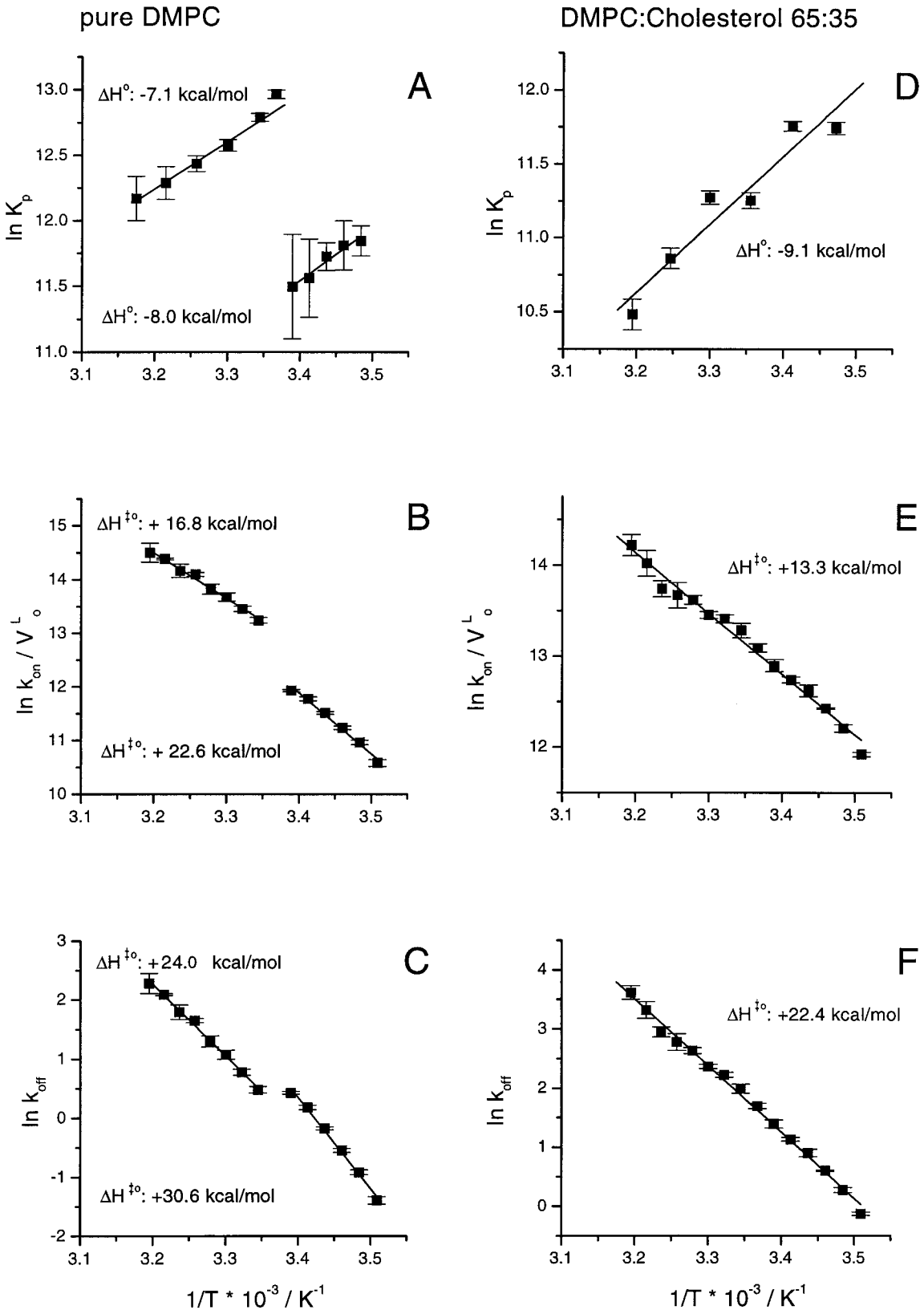

FIGURE 5 Single-phase vesicles. Van't Hoff (*A, D*) and Arrhenius (*B, C, E, F*) plots are used to determine standard enthalpies and standard enthalpies of activation for the insertion of U-6 into the different phases (see text). Low-temperature points are shown in *A*, *B*, and *C*: *s* phase. High-temperature points are shown in *A*, *B*, and *C*: ℓ_d phase. *D*, *E*, *F*: ℓ_o phase.

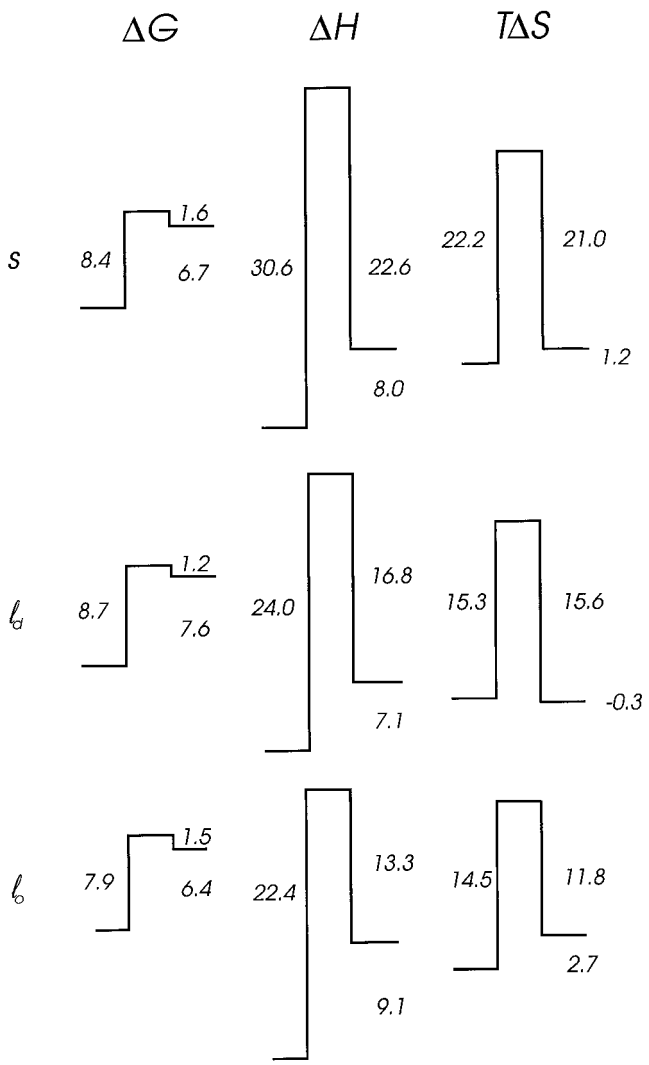

FIGURE 6 Single-phase vesicles: graphical summary of the thermodynamic analysis. Each picture contains information on the equilibrium state and Gibbs energies, enthalpies, and entropies of activation (in kcal/mol) for both insertion and desorption for each phase investigated. The right-hand side always refers to the probe in water, the left-hand side to the probe inserted into the lipid bilayer (compare Fig. 9).

(Fig. 1) are clearly two exponential on the time scale of the experiment (*empty circles* in Fig. 7 *C*), similar to the data points obtained in pure DMPC vesicles close to the T_m. The faster exponential is of an order of magnitude that would be expected from the single-phase data, but the slower exponential is of an order of magnitude faster than predicted.

Taking a closer look at the rates involved, we find that the time frame of desorption from both liquid phases is sufficiently long to allow lateral diffusion of the probe molecules over the entire vesicle surface before desorption. This would imply that the probe molecules would desorb from an equilibrium distribution and not necessarily from the phase into which they inserted. The simple reaction scheme presented here for the two-phase system does not take into account diffusion of probe within the bilayer, but we can estimate its effect on $-\lambda_2$. From the values for K_p determined for each phase in single-phase vesicles we can predict the partition coefficient between the two lipid phases ℓ_d and ℓ_o, $K_p^{\ell_d\text{-}\ell_o}$, which is given by the ratio of the two lipid-water partition coefficient in the two phases: $K_p^{\ell_d\text{-}\ell_o} = K_p^{\ell_d}/K_p^{\ell_o}$. We find that the probe partitions preferentially into the ℓ_d phase with a $K_p^{\ell_d\text{-}\ell_o} = 4.8$. To obtain a lower limit for $-\lambda_2$, we can therefore assume that all probe molecules come off the same phase with the same rate, $k_{off}^a = k_{off}^b$. The corresponding change in the magnitude of λ_2, however, is on the order of 5%.

The same analysis was performed for the kinetic traces obtained in the region of s-ℓ_o coexistence (Fig. 7 *B, dots*). In this case, however, the theoretical curve obtained with the values for the pure phases (*solid line* in Fig. 7 *B*) does not describe the experimental data. In general we find the experimental kinetics to be significantly slower than predicted on the basis of the rates for pure *s*- and pure ℓ_o-phase vesicles (see *low temperature points* in Fig. 7 *C*). The partition coefficient between the *s* and ℓ_o phases calculated from the data on single-phase vesicles is close to 1, which may be an underestimate, because of probe molecules located in grain boundary defects in pure *s*-phase vesicles. In a region of s-ℓ_o coexistence, however, pure *s*-phase domains are much smaller and, therefore, more likely to be free of packing defects. In this case the probe molecules could be largely excluded from the pure solid phase and partition preferentially into the ℓ_o phase. However, even with this correction we have to assume an on-rate into the ℓ_o phase that is an order of magnitude slower than that obtained from the analysis of the pure ℓ_o-phase vesicles or a much larger fraction of *s* phase to describe the experimental traces.

Another indication that vesicles composed of coexisting ℓ_o and *s* phases do not behave as predicted on the basis of their phase composition and the results from pure-phase vesicles stems from the measurement of the relative fluorescence intensities as a function of phase. Fig. 8 shows a plot of the relative fluorescence intensities in vesicles in the *s*, ℓ_d, ℓ_o phase, and in two-phase vesicles. In the ℓ_d-ℓ_o coexistence region we find that the relative fluorescence intensities agree within the experimental error with the average intensities in the two individual phases, weighted by the fraction of phases (*solid line* in Fig. 8). In the region of s-ℓ_o coexistence, however, the relative fluorescence intensities coincide with the values measured in the pure *s* phase rather than with the weighted averages calculated from the fluorescence intensities of the ℓ_o and *s* phase.

DISCUSSION

Single-phase vesicles

To answer the question of how interfacial regions present in phase-separated systems influence the kinetics and equilib-

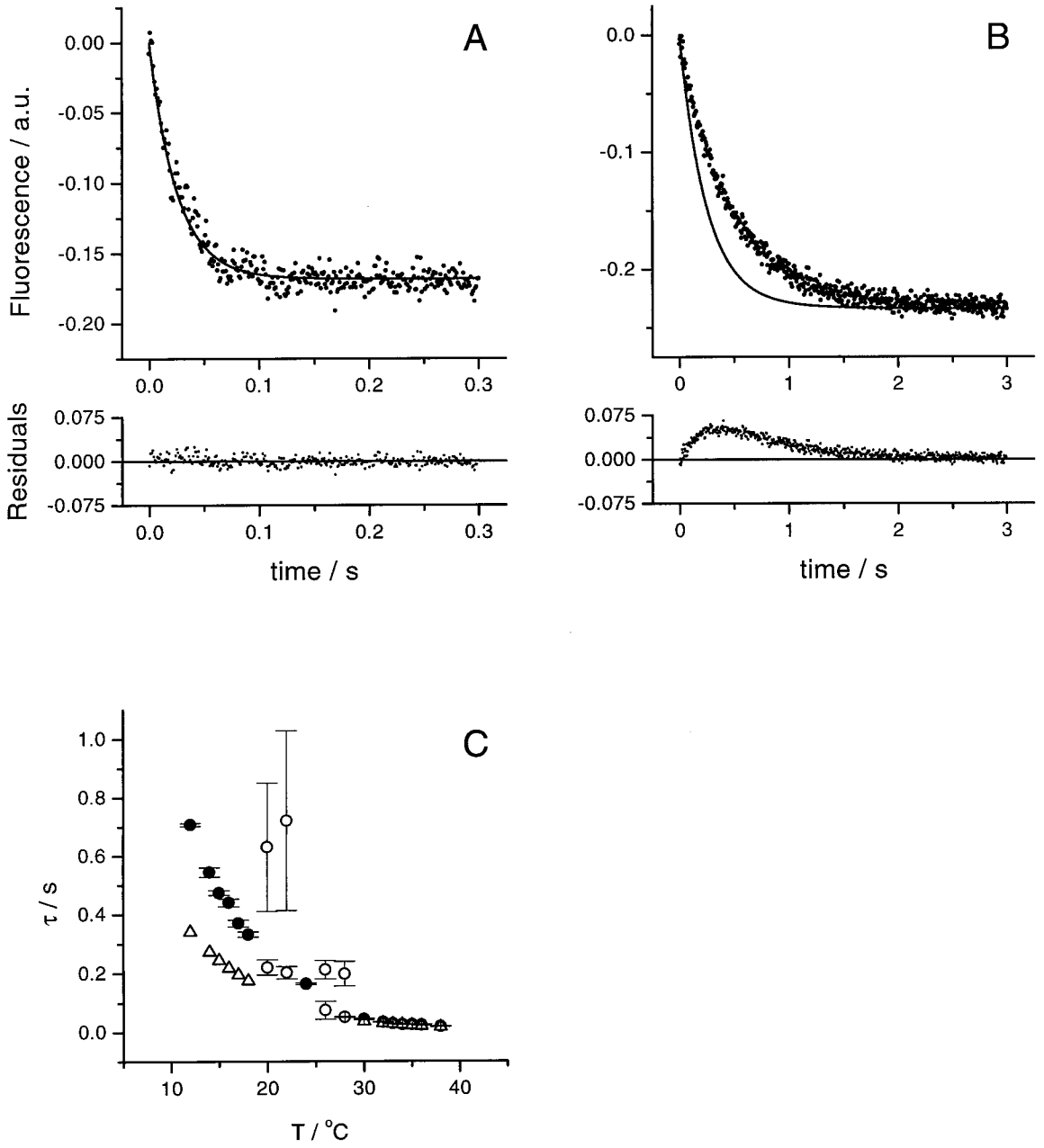

FIGURE 7 Two-phase vesicles. (*A*) —, Theoretical prediction for the kinetics of association of U-6 with vesicles in a region of ℓ_d-ℓ_o phase coexistence: $f_{\ell_d} = 0.74$, $k_{on}^{\ell_d} = 7.74 \times 10^5\ s^{-1}\ M^{-1}$, $k_{off}^{\ell_d} = 4.81\ s^{-1}$, $k_{on}^{\ell_o} = 5.46 \times 10^5\ s^{-1}\ M^{-1}$, $k_{off}^{\ell_o} = 17.62\ s^{-1}$. $-1/\lambda_1 = 0.231$ s, $-1/\lambda_2 = 0.02528$ s. ●, Experimental data obtained using LUVs containing 15% cholesterol at 34°C ($f_{\ell_d} = 0.74$). (*B*) —, Theoretical prediction for the kinetics of association of U-6 with vesicles in a region of *s*-ℓ_o phase coexistence: $f_s = 0.62$, $k_{on}^{s} = 3.70 \times 10^4\ s^{-1}\ M^{-1}$, $k_{off}^{s} = 0.466\ s^{-1}$, $k_{on}^{\ell_o} = 1.26 \times 10^5\ s^{-1}\ M^{-1}$, $k_{off}^{\ell_o} = 1.56\ s^{-1}$. $-1/\lambda_1 = 2.62$ s, $-1/\lambda_2 = 0.247$ s. ●, Experimental data obtained using LUVs containing 15% cholesterol at 15°C ($f_s = 0.62$). (*C*) ●, Time constants (τ_{obs}) as obtained from a monoexponential fit to the experimental data and their standard deviation ($n = 6$). ○, τ_1 and τ_2 as obtained from a two-exponential fit to the experimental data at temperatures close to the solidus line. △, The values of $-1/\lambda_2$ obtained from Eq. 12, using the parameters from single-phase vesicles, as exemplified in *A* and *B*.

ria of association of small amphiphiles with two phase lipid bilayers, we first need to form a clear picture of the probe behavior in the pure phases. Amphiphile partitioning has been studied in some detail before (e.g., Duckwitz-Peterlein et al., 1977; Frank et al., 1983; Nichols, 1985), and the general picture is well known. What is new in this study is that we gain a very detailed idea of how different lipid phases influence amphiphile partitioning, including the ℓ_o phase, which may be of biological relevance. The kinetic analysis we present here allows us to determine the ther-

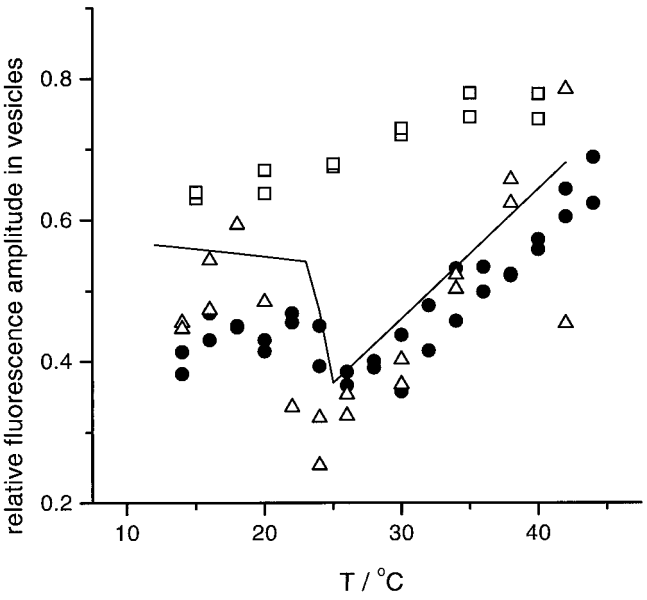

FIGURE 8 Fluorescence intensity of U-6 inserted into vesicles relative to the intensity in buffer. ●, Vesicles containing 15% cholesterol. □, Vesicles containing 35% cholesterol. △, Pure DMPC vesicles. —, Averaged intensities between the values obtained from pure DMPC vesicles and vesicles composed of DMPC : cholesterol 65 : 35, weighted by the fractional amounts of phases present at each temperature.

modynamic quantities associated with the incorporation of probe into lipid bilayer vesicles and how these quantities vary with lipid phase.

We did not specifically include charge effects in the analysis, although at the experimental pH of 8.5 ~50% of the probe molecules carry a net positive charge when incorporated into the vesicles. The accumulation of positive charges in the vesicles could influence both insertion and desorption of probe molecules and lead to an apparent time dependence of the observed rate constants. But we would then see a deviation from simple monoexponential kinetics, which is clearly not the case. The simple model that we use here is thus sufficient to account for the experimental results. One explanation for this observation may lie in the fact that the maximum charge density in the vesicles due to the incorporation of fluorophore will always be small, because the concentration of charged species in the bilayer can never exceed 2.5 mol%. Its influence on the process of desorption due to repulsion of like charges can, therefore, be expected to be negligible. Similarly, because of its low charge density, the membrane will interact only weakly with charges in solution. Moreover, at pH 8.5, most probe molecules in solution are zwitterionic, with only ~10% carrying a net positive charge. Therefore, the effect of membrane charge on the on-rate is expected to be very small.

There has been considerable discussion in the literature over the use of an association or binding constant versus a partition coefficient in the description of amphiphile association with membranes (White et al., 1998). It is therefore of interest to point out that it does not matter whether we use K_p or K_a in the kinetic description because k_{obs} does not depend on lipid molar volume. The criticism has been raised that the formulation of amphiphile association with lipid bilayers in terms of binding (reaction scheme 1) would automatically entail a 1 : 1 stoichiometry and, therefore, the "consumption" of lipid. However, this interpretation is merely a consequence of the formalism chosen to depict the reaction and does not present a real problem because we explicitly keep the lipid concentration constant in Eq. 2. Therefore, $k_{on}[L]$ becomes a pseudo-first-order rate constant. Moreover, it has been stated that a treatment in terms of binding would involve the definition of binding sites, which, in the case of vesicles, is a poorly defined concept. However, as will be shown shortly, we may think of probe binding as occurring per unit volume, which we take as the volume accessible to the probe molecule in the lipid bilayer. For low concentrations of probe we can then consider a vesicle to consist of an infinite number of binding "sites" to which binding occurs independently of how many probe molecules are already bound (or still to be bound). It is important to note that this treatment is only valid for low concentrations of probe. This restriction, however, applies equally to a treatment in terms of a partition coefficient because the latter will also change at higher probe concentrations. It is only in the thermodynamic treatment that we are restricted to the use of K_p to obtain Gibbs energies, enthalpies, and entropies that reflect only the difference in interactions between a probe molecule in water versus a probe molecule in a lipid bilayer (see Ben-Naim, 1978, for a detailed discussion of this point).

The result of the thermodynamic analysis is summarized graphically in Fig. 6. To facilitate comparison between the actual magnitudes of the constants, all values have been extrapolated to 24°C. We find that the probe partitions preferentially into the ℓ_d phase, and basically to the same degree into either the ℓ_o or the s phase. The surprisingly low partition coefficient despite the high enthalpy for insertion observed for the ℓ_o phase is due to a small but significant unfavorable contribution of $T\Delta S^o$ to the ΔG^o for insertion (see below). Nevertheless, we find that the process of insertion is entirely driven by enthalpy and not by an increase in entropy, as could be expected on the basis of the hydrophobic effect. An enthalpy-driven partitioning into membranes has been found for a number of compounds (Huang and Charlton, 1972; Nichols, 1985; Seelig and Ganz, 1991) and recognized as being emphasized in the partitioning of charged amphiphiles into phospholipid bilayers (Bäuerle and Seelig, 1991).

Let us next examine the thermodynamics of insertion and desorption in some detail. The generally large magnitudes of $\Delta S^{\ddagger o}$ and $\Delta H^{\ddagger o}$ for insertion and desorption suggest that they contain significant contributions both from electrostatic interactions and the hydrophobic effect. Consider first

the process of insertion. $\Delta G^{\ddagger o}_{on}$ shows rather little dependence on lipid phase and lies between 1.2 and 1.6 kcal/mol at 24°C. At higher temperatures $T\Delta S^{\ddagger o}_{on}$ will contribute relatively more to $\Delta G^{\ddagger o}_{on}$, so that we can then expect insertion to become essentially diffusion limited. To fully interpret the values of $\Delta G^{\ddagger o}_{on}$, we must consider the individual contributions of $\Delta H^{\ddagger o}_{on}$ and $T\Delta S^{\ddagger o}_{on}$ to $\Delta G^{\ddagger o}_{on}$.

Removing the probe from water will liberate water tightly bound to the probe "head," which is enthalpically unfavorable, whereas removal of the acyl chain from water is enthalpically neutral at room temperature (Kauzmann, 1959). However, forming the activated state also involves disrupting hydrogen bonds and other interactions in the membrane-water interfacial layer, which is probably a structured region with properties quite different from those of the bulk phases (Fig. 9). The disruption of this interfacial layer can be expected to cost the most energy in the most ordered phase. We find the highest $\Delta H^{\ddagger o}_{on}$ for insertion into the *s* phase, which supports this interpretation. Interestingly, from a thermodynamic analysis of the binding of small peptides to bilayers, Jacobs and White (1989) found that 60–70% of the hydrophobic effect contribution to this process corresponds to peptide binding to the membrane-water interface.

The lowest $\Delta H^{\ddagger o}_{on}$ is associated with insertion into the ℓ_o phase, which is indicative of weaker molecular interactions in the lipid-water interface as compared to either the ℓ_d or the *s* phase. $\Delta S^{\ddagger o}_{on}$ follows the same trend. Removal of the probe from water is an entropically favorable process close to room temperature and independent of lipid phase. This would account for a $T\Delta S^{\ddagger o}_{on}$ independent of lipid phase, which is clearly not what we observe (Fig. 6). However, disrupting the membrane-water interfacial layer will introduce a dependence of $T\Delta S^{\ddagger o}_{on}$ on lipid phase. We find that $T\Delta S^{\ddagger o}_{on}$ is largest for the *s* phase and smallest for the ℓ_o phase, suggesting that the order of the interfacial layer follows the same sequence.

Consider next the process of desorption. Here we find that $\Delta G^{\ddagger o}_{off}$ from the bilayer is lowest in the ℓ_o phase, corresponding to the fastest off-rate (5 s^{-1}), and highest from the ℓ_d phase (k_{off} = 1.3 s^{-1}). Looking at the contribution of $\Delta H^{\ddagger o}_{off}$ to $\Delta G^{\ddagger o}_{off}$, we find that desorption from all phases is associated with a large enthalpy of activation. Its contribution is highest in the *s* phase, indicative of strong lipid-probe interactions, and lowest in the ℓ_o phase. We find a value of 24 kcal/mol for $\Delta H^{\ddagger o}_{off}$ in the ℓ_d phase, and 30.6 kcal/mol in the *s* phase. These values coincide with the values of 24.9 kcal/mol and 31.7 kcal/mol Wimley and Thompson observed for the desorption of DMPC monomers from DMPC vesicles in the ℓ_d and *s* phases (Wimley and Thompson, 1990). They are, however, ~10 kcal/mol higher than observed for desorption of [^{3}H]palmitoyloleoylphosphatidylcholine ([^{3}H]POPC) from small unilamellar POPC vesicles (Jones and Thompson, 1990) and *N*-7-nitrobenz-2-oxa-1,3-diazol-4-yl-amino chain-labeled phosphatidylcholines from DOPC vesicles (Nichols, 1985). In both cases lipid-lipid interactions in the inserted state are probably weakened by either strained lipid packing in small unilamellar vesicles or the presence of a bulky chain label, making desorption energetically more favorable.

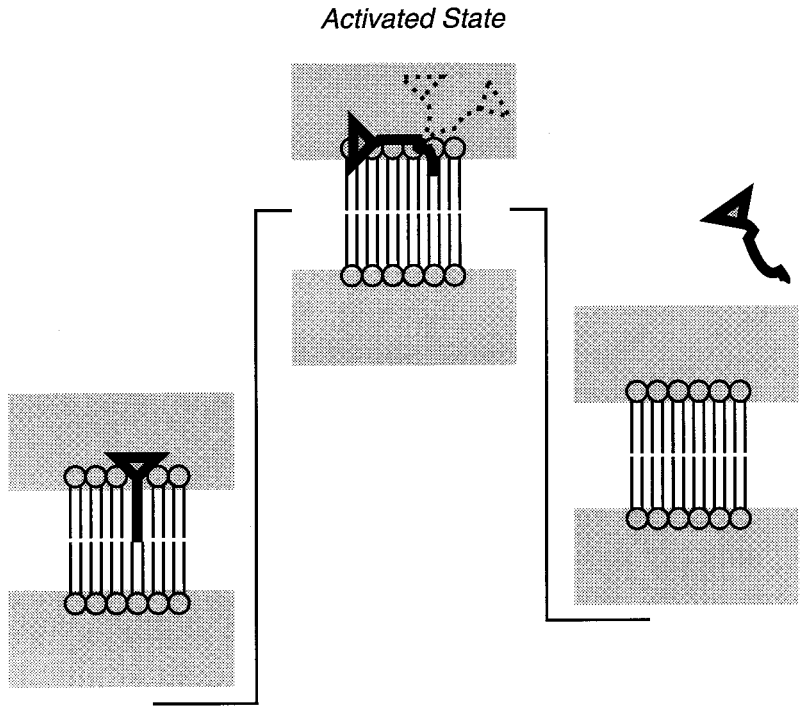

FIGURE 9 Schematic representation of the activated state model used in the Discussion. The dotted outlines of the probe molecule in the activated state are meant to indicate a considerable amount of motional freedom as compared to the completely inserted state. The shaded area refers to an interfacial region that has properties different from those of bulk water (see text).

We find that the entropies of activation follow the same trend as the enthalpies of activation, being highest for desorption from the *s* phase and lowest for desorption from the ℓ_o phase. It is difficult to relate these values to published ones because the exact values for $T\Delta S^{\ddagger o}$ depend on the particular activated-state model used in the determination of $\Delta G^{\ddagger o}$ (see Results). The high values we find for $T\Delta S^{\ddagger o}_{off}$ are presumably due to the disruption of the membrane-water interfacial layer and the restricted mobility of the probe itself in the membrane as compared to the activated state, making desorption from the *s* phase entropically most favorable. We would like to point out that this interpretation does not follow the widely held notion that the slow lipid off-rates are primarily due to the hydrophobic effect, i.e., to an unfavorable entropy change associated with the transfer of a lipid to the aqueous phase (Aniansson et al., 1976; Nichols, 1985; Jones and Thompson, 1990; Wimley and Thompson, 1990, 1991). The differences we find between $T\Delta S^{\ddagger o}_{off}$ and $T\Delta S^{\ddagger o}_{on}$ are generally very small, so that we may conclude that the favorable gain in entropy associated with removal of the probe from water is basically compensated for by the loss of entropy associated with the insertion into the highly anisotropic membrane.

In this context it is interesting to note that insertion into the ℓ_o phase is, in fact, associated with a small but unfavorable overall change in entropy ($\Delta S^o = -9$ cal mol^{-1} K^{-1}). DeYoung and Dill observed that increasing cholesterol concentrations led to successively lower membrane-water partition coefficients of benzene (DeYoung and Dill, 1988). They attributed this effect to a lowering of the area per phospholipid in the presence of high amounts of cholesterol, leading to an entropic exclusion of solute from the bilayer. In this case we would expect to find a higher value for $T\Delta S^{\ddagger o}_{off}$ for desorption from the ℓ_o phase than from the ℓ_d phase, reflecting the smaller area per phospholipid in the ℓ_o phase and a correspondingly more favorable $T\Delta S^{\ddagger o}_{off}$. However, comparing the ℓ_o with the ℓ_d phase, we find that the values for $T\Delta S^{\ddagger o}_{off}$ are actually very similar for the two fluid phases (14.5 versus 15.3 kcal/mol) and, thus, are quite independent of cholesterol content. A closer look shows that the unfavorable overall entropy change associated with the ℓ_o phase is, in fact, due to a lowered entropy of activation connected with removing the probe from water. In this case it seems more appropriate to attribute the unfavorable entropy change to an interfacial layer that is less ordered in the ℓ_o than in the ℓ_d phase. The interpretations given above can be summarized in a model of the activated state that is given in Fig. 9. We think of the activated state as a state in which the probe is loosely associated with the membrane but still possesses considerable motional freedom. Large parts of the probe would then be, in fact, removed from both bulk water and the membrane but in contact with a layer of structured water adjacent to the bilayer with distinct properties (Leikin et al., 1993), as represented by the hatched areas in Fig. 9.

With this picture in mind we can try to rationalize the observation of two-exponential kinetics at temperatures close to the T_m in pure DMPC vesicles (22–24°C). First of all, two-exponential kinetics point toward the existence of more than one phase within the time frame of the experiment at these temperatures. Second, the rate of desorption from DMPC vesicles at these temperatures must be significantly faster than from either the ℓ_d or the *s* phase. If the probe was desorbing from the membrane with a combination of off-rates from the ℓ_d and the *s* phase, we would expect to find a second slow exponential on the order of several seconds (as mentioned in the analysis of two-phase vesicles), which we would not be able to detect on the time scale of the experiment. A fast rate of desorption signifies a low $\Delta G^{\ddagger o}_{off}$, which can only be accounted for by a drastically altered membrane structure around the T_m that facilitates desorption. Third, the faster of the two observed relaxation times lies well within what we would expect for insertion into an ℓ_d-*s* mixed-phase region, indicating that insertion is influenced relatively little by the structure of the membrane itself.

Two-phase vesicles

We can think of an interface between two phases coexisting in the plane of the bilayer as being formed at the expense of one or both phases present. If the total amount of interface were small, we would expect its effects on the kinetic of association to be negligible. We should then be able to describe the overall kinetics simply by using a combination of the individual rates corresponding to each of the two phases involved according to the equations derived here for a two-phase system. We believe this to be case for an ℓ_o-ℓ_d mixed-phase system where the data from the single-phase vesicles suffice to account for the kinetics in the region of phase coexistence. It is thus unlikely that the insertion of small amphiphiles will be facilitated by phase separations of this kind.

The interesting observation of a second exponential detectable on the experimental time scale at temperatures around the solidus (*horizontal*) line (Fig. 1) in vesicles containing 15 mol% cholesterol can, again, only be accounted for by fast rates of desorption, in analogy to the interpretation of two-exponential kinetics observed in pure DMPC vesicles close to the T_m, as given above. The magnitude of the faster of the two apparent rate constants, $-\lambda_2$, is dominated by the two on-rates, and if these are little affected, $-\lambda_2$ will be within the same order of magnitude as predicted based on the analysis presented here. However, the slower relaxation time, $-\lambda_1$, is dominated by the desorption rates, and if these become much faster at temperatures close to the solidus line we would expect $-\lambda_1$ to change accordingly. We can thus conclude that the bilayer structure at these temperatures is very different from the one

that exists at temperatures well below or above the solidus line, making probe desorption much more favorable.

Our results on the ℓ_o-ℓ_d mixed-phase system are somewhat in contrast to previous reports of increased efflux of ions and small molecules from phosphatidylcholine vesicles containing ~20 mol% cholesterol, which was attributed to lipid packing defects at the phase boundaries in regions of phase coexistence (Corvera et al., 1992; Xiang and Anderson, 1998). Such defect structures could, in principle, also be detected through our experiments, as they can be expected to lead to faster kinetics of association and altered equilibrium binding. However, one must keep in mind that these defects have a finite lifetime. In efflux experiments the vesicles are loaded with a very high concentration of permeant, so that the distance through which the permeant has to diffuse before hitting the bilayer becomes very small. If the diffusion coefficient of the permeant in water is such that the time it takes to reach the membrane is smaller than or on the same order as the lifetime of a defect structure in the bilayer, the permeability of the bilayer will, in fact, appear to be increased. The lifetime of these defects can be estimated from the translational diffusion hopping rate of a phospholipid molecule, which is on the order of 10^7 s^{-1} at room temperature in a fluid phase (Clegg and Vaz, 1985). To reach the bilayer within $\sim 10^{-7}$ s, we require a probe concentration at least on the order of 10^{-3} M. For a probe concentration in the micromolar range, however, the characteristic time for the diffusion-controlled encounter of probe molecules with the membrane can be estimated to be $\sim 10^{-5}$ s at room temperature. Short-lived defects on the order of 10^{-7} s will thus go undetected in our insertion experiments. We can then conclude that the apparent permeability of a lipid bilayer will also depend on the type of experiment we choose to investigate it with, or, in other words, a membrane may appear quite tight to a small amphiphile in dilute solution and quite permeable to an ion whose activity close to the membrane is very high.

In the ℓ_o-*s* phase coexistence region the picture appears quite different. Using the kinetic data from the analysis of single-phase vesicles and the mole fractions of phases from the phase diagram in Fig. 1 does not result in an adequate description of the experimentally observed kinetics, which are significantly slower than expected. We believe that this is due to an order decay over a large coherence length from the *s* to the ℓ_o phase, leading to an effective ordering of the ℓ_o phase, in a way similar to what has been proposed to lead to slower diffusion of lipids in the bilayer in the presence of proteins or gel-phase domains (Almeida et al., 1992b). Such a system could be expected to be much more "solid-like" than predicted from the phase diagram and, in the extreme case, approach pure *s*-phase kinetics. Interestingly, the kinetics of association in the ℓ_o-*s* coexistence region are even slower than in pure solid-phase vesicles. We believe this to be due to a better lipid packing in the *s*-phase domains, which, being smaller than in pure *s*-phase vesicles, are more likely to be free of packing defects, as well as to a higher degree of order in the ℓ_o-phase domains in the mixed-phase system. The presence of ℓ_o-*s*-phase boundaries thus seems to prevent the insertion of small amphiphiles rather than promoting it.

REFERENCES

Almeida, P. F. F. 1999. Lipid transfer between vesicles: effect of high vesicle concentration. *Biophys. J.* 76:1922–1928.

Almeida, P. F. F., W. L. C. Vaz, and T. E. Thompson. 1992a. Lateral diffusion in the liquid phases of dimyristoylphosphatidylcholine/cholesterol lipid bilayers: a free volume analysis. *Biochemistry.* 31: 6739–6747.

Almeida, P. F. F., W. L. C. Vaz, and T. E. Thompson. 1992b. Lateral diffusion and percolation in two-phase, two-component lipid bilayers. Topology of the solid-phase domains in-plane and across the lipid bilayer. *Biochemistry.* 31:7198–7210.

Aniansson, E. A. G., S. H. Wall, M. Almgren, H. Hoffman, I. Kielmann, W. Ulbricht, R. Zana, J. Lang, and C. Tondre. 1976. Theory of the kinetics of micellar equilibria and quantitative interpretation of chemical relaxation studies of micellar solutions of ionic surfactants. *J. Phys. Chem.* 80:905–922.

Bäuerle, H.-D., and J. Seelig. 1991. Interaction of charged and uncharged calcium channel antagonists with phospholipid membranes. Binding equilibrium, binding enthalpy, and membrane location. *Biochemistry.* 30:7203–7211.

Ben-Naim, A. 1978. Standard thermodynamics of transfer. Uses and misuses. *J. Phys. Chem.* 82:792–803.

Boas, M. L. 1983. Linear equations, vectors, matrices, and determinants, Chap. 3, and Coordinate transformations, tensor analysis, Chap. 10. *In* Mathematical Methods in the Physical Sciences, 2nd Ed. John Wiley and Sons, New York. 81–144 and 407–455.

Brown, D. and J. K. Rose. 1992. Sorting of GPI-anchored proteins to glycolipid-enriched membrane subdomains during transport to the apical cell surface. *Cell.* 68:533–544.

Clegg, R. M., and W. L. C. Vaz. 1985. Translational diffusion of proteins and lipids in artificial lipid bilayer membranes. A comparison of experiment with theory. *In* Progress in Protein-Lipid Interactions 1. A. Watts and J. J. H. H. M. DePont, editors. Elsevier, Amsterdam. 173–229.

Clerc, S., and T. E. Thompson. 1995. Permeability of dimyristoylphosphatidylcholine/dipalmitoylphosphatidylcholine bilayer membranes with coexisting gel and liquid-crystalline phases. *Biophys. J.* 68:2333–2341.

Corvera, E., O. G. Mouritsen, M. A. Singer, and M. J. Zuckermann. 1992. The permeability and the effect of acyl-chain length for phospholipid bilayers containing cholesterol: theory and experiment. *Biochim. Biophys. Acta.* 1107:261–270.

Cruzeiro-Hansson, L., and O. G. Mouritson. 1988. Passive ion permeability of lipid membranes modelled via lipid-domain interfacial area. *Biochim. Biophys. Acta.* 944:63–72.

Cullis, P. R., and M. J. Hope. 1985. Physical properties and functional roles of lipids in membranes. *In* Biochemistry of Lipids and Membranes. D. E. Vance and J. E. Vance, editors. Benjamin/Cummings, Menlo Park, CA. 28–33.

DeYoung, L. R., and K. A. Dill. 1988. Solute partitioning into lipid bilayer membranes. *Biochemistry.* 27:5281–5289.

Duckwitz-Peterlein, G., G. Eilenberger, and P. Overath. 1977. Phospholipid exchange between bilayer membranes. *Biochim. Biophys. Acta.* 469:311–325.

Edidin, M. 1997. Lipid microdomains in cell surface membranes. *Curr. Opin. Struct. Biol.* 7:528–532.

Frank, A., Y. Barenholz, D. Lichtenberg, and T. E. Thompson. 1983. Spontaneous transfer of sphingomyelin between phospholipid bilayers. *Biochemistry.* 22:5647–5651.

Gutfreund, H. 1995. Kinetics for the Life Sciences. Receptors, Transmitters and Catalysts. Cambridge University Press, Cambridge. 112–118.

Huang, C.-H., and J. P. Charlton. 1972. Interactions of phosphatidylcholine vesicles with 2-*p*-toluidinylnaphthalene-6-sulfonate. *Biochemistry.* 11: 735–740.

Hwang, J., L. A. Gheber, L. Margolis, and M. Edidin. 1998. Domains in cell plasma membranes investigated by near-field scanning optical microscopy. *Biophys. J.* 74:2184–2190.

Ipsen, H. J., G. Karlström, O. G. Mouritsen, H. Wennerström, and M. J. Zuckermann. 1987. Phase equilibria in the phosphatidylcholine-cholesterol system. *Biochim. Biophys. Acta.* 905:162–172.

Jacobs, R. E., and S. H. White. 1989. The nature of the hydrophobic binding of small peptides at the bilayer interface: implications for the insertion of transbilayer helices. *Biochemistry.* 28:3421–3427.

Jones, J. D., and T. E. Thompson. 1990. Mechanism of spontaneous, concentration-dependent phospholipid transfer between bilayers. *Biochemistry.* 29:1593–1600.

Kauzmann, W. 1959. Some factors in the interpretation of protein denaturation. *Adv. Protein Chem.* 14:1–63.

Kenworthy, A. K., and M. Edidin. 1998. Distribution of a glycosylphosphatidylinositol-anchored protein at the apical surface of MDCK cells examined at a resolution of 100 Å using imaging fluorescence resonance energy transfer. *J. Cell Biol.* 142:69–84.

Kraayenhof, R., G. J. Sterk, and H. W. Wong Fong Sang. 1993. Probing biomembrane interfacial potential and pH profiles with a new type of float-like fluorophores positioned at varying distance from the membrane surface. *Biochemistry.* 32:10057–10066.

Kurzchalia, T. V., E. Hartmann, and P. Dupree. 1995. Guilt by insolubility—does a protein's detergent insolubility reflect a caveolar location? *Trends Cell Biol.* 5:187–189.

Leikin, S., V. A. Parsegian, D. C. Rau, and R. P. Rand. 1993. Hydration forces. *Annu. Rev. Phys. Chem.* 44:369–395.

Lisanti, M. P., P. E. Scherer, Z. Tang, and M. Sargiacomo. 1994. Caveolae, caveolin and caveolin-rich membrane domains: a signalling hypothesis. *Trends Cell Biol.* 4:231–235.

Marsh, D., A. Watts, and P. F. Knowles. 1976. Evidence for phase boundary lipid. Permeability of Tempo-choline into dimyristoylphosphatidylcholine vesicles at the phase transition. *Biochemistry.* 15:3570–3578.

Mayor, S., and F. R. Maxfield. 1995. Insolubility and redistribution of GPI-anchored proteins at the cell surface after detergent treatment. *Mol. Biol. Cell.* 6:929–944.

Melo, E. C., I. M. Lourtie, M. B. Sankaram, T. E. Thompson, and W. L. C. Vaz. 1992. Effects of domain connection and disconnection on the yields of in-plane bimolecular reactions in membranes. *Biophys. J.* 63: 1506–1512.

Nichols, J. W. 1985. Thermodynamics and kinetics of phospholipid monomer-vesicle interaction. *Biochemistry.* 24:6390–6398.

Papahadjopoulos, D., K. Jacobson, S. Nir, and T. Isac. 1973. Phase transitions in phospholipid vesicles. Fluorescence polarization and permeability measurements concerning the effect of temperature and cholesterol. *Biochim. Biophys. Acta.* 311:330–348.

Sankaram, M. B., and T. E. Thompson. 1990. Interaction of cholesterol with various glycerophospholipids and sphingomyelin. *Biochemistry.* 29:10670–10675.

Sankaram, M. B., and T. E. Thompson. 1991. Cholesterol-induced fluid-phase immiscibility in membranes. *Proc. Natl. Acad. Sci. USA.* 88: 8686–8690.

Seelig, J., and P. Ganz. 1991. Nonclassical hydrophobic effect in membrane binding equilibria. *Biochemistry.* 30:9354–9359.

Simons, K., and E. Ikonen. 1997. Functional rafts in cell membranes. *Nature.* 387:569–572.

Smoluchowski, M. 1917. Versuch einer mathematischen Theorie der Koagulationskinetik kolloider Lösungen. *Z. Physik. Chem. Leipzig.* 92: 129–168.

Thompson, T. E., M. B. Sankaram, R. L. Biltonen, D. Marsh, and W. L. Vaz. 1995. Effects of domain structure on in-plane reactions and interactions. *Mol. Membr. Biol.* 12:157–162.

Vaz, W. L. C. 1994. Diffusion and chemical reactions in phase-separated membranes. *Biophys. Chem.* 50:139–145.

Vaz, W. L. C. 1995. Percolation properties of two-component, two-phase phospholipid bilayers. *Mol. Membr. Biol.* 12:39–43.

Vaz, W. L. C. 1996. Consequences of phase separations in membranes. *In* Non-Medical Applications of Liposomes, Vol. 2, Models for Biological Phenomena. Y. Barenholz and D. Lasic, editors. CRC Press, Boca Raton, FL. 51–60.

Vaz, W. L. C., and P. F. F. Almeida. 1993. Phase topology and percolation in multi-phase lipid bilayers: is the biological membrane a domain mosaic? *Curr. Opin. Struct. Biol.* 3:482–488.

Vist, M. R., and J. H. Davis. 1990. Phase equilibria of cholesterol/dipalmitoylphosphatidylcholine mixtures: ^{2}H nuclear magnetic resonance and differential scanning calorimetry. *Biochemistry.* 29:451–464.

Welti, R., and M. Glaser. 1994. Lipid domains in model and biological membranes. *Chem. Phys. Lipids.* 73:121–137.

White, S., W. C. Wimley, A. S. Ladokhin, and K. Hristova. 1998. Protein folding in membranes: determining energetics of peptide-bilayer interactions. *Methods Enzymol.* 295:63–87.

Wimley, W. C., and T. E. Thompson. 1990. Exchange and flip-flop of dimyristoylphosphatidylcholine in liquid-crystalline, gel, and two-component, two-phase large unilamellar vesicles. *Biochemistry.* 29: 1296–1303.

Wimley, W. C., and T. E. Thompson. 1991. Transbilayer and interbilayer phospholipid exchange in dimyristoylphosphatidylcholine/dimyristoylphosphatidylethanolamine large unilamellar vesicles. *Biochemistry.* 30:1702–1709.

Wu, H. S., and H. M. McConnell. 1975. Phase separations in phospholipid membranes. *Biochemistry.* 14:847–854.

Xiang, T.-X., and B. D. Anderson. 1998. Phase structures of binary lipid bilayers as revealed by permeability of small molecules. *Biochim. Biophys. Acta.* 1370:64–76.